Talanta 117 (2013) 81–86

Contents lists available at ScienceDirect

Talanta

journal homepage: www.elsevier.com/locate/talanta

A reusable and sensitive biosensor for total mercury in canned fish based on fluorescence polarization

Tongfei Shen [a], Qiaoli Yue [a,*], Xiuxiu Jiang [a], Lei Wang [a], Shuling Xu [a], Haibo Li [a], Xiaohong Gu [b], Shuqiu Zhang [b], Jifeng Liu [a,*]

[a] Department of Chemistry, Liaocheng University, Liaocheng 252059, PR China
[b] Shandong Provincial Key Lab of Test Technology on Food Quality and Safety, Shandong Academy of Agricultural Sciences, Jinan 250100, PR China

ARTICLE INFO

Article history:
Received 23 April 2013
Received in revised form
12 August 2013
Accepted 14 August 2013
Available online 30 August 2013

Keywords:
Mercury
Magnetic nanoparticles
Fluorescence Polarization
Canned fish

ABSTRACT

In this work, we developed a sensitive and selective sensor technique for total mercury (Hg) detection in canned fish samples based on the fluorescence polarization (FP) method. The detection principle was that ssDNA containing thymine (T) bases was modified on magnetic nanoparticles (MNPs), which were used as enhancement probe. In the presence of Hg^{2+}, the ssDNA on MNPs can hybridize with the fluorophore labeled aptamer owing to the specific interaction between T bases and Hg^{2+}. The formation of thymine–Hg^{2+}–thymine (T–Hg^{2+}–T) complexes leads to the molar mass increase of fluorophore molecules, resulting in the enhancement of FP signal. The increase of FP was in a good linearity with the concentration of Hg^{2+} in range of 2.0 nM–1.0 mM and the limit of detection was 0.49 nM (3.29 S_B/m, according to the recent recommendation of IUPAC). Moreover, the proposed biosensor can be reused for 6 cycling times and was successfully applied in monitoring Hg^{2+} in real samples.

1. Introduction

Fluorescence polarization (FP) is a powerful technique for the homogeneous analysis of molecular interactions, which was first proposed in 1926 by Perrin [1]. Subsequently, Weber's theoretical and experimental work extended Perrin's earlier contributions and developed modern FP instrumentation [2]. Based on the principle of photoselective excitation of a population of fluorophores using polarized radiation, FP of a molecule is proportional to the molecule's rotational relaxation time. From FP measurements valuable information on molecular orientation, mobility and processes for biological interactions can be obtained. Since the establishment of the theory and method, FP has been a valuable biophysical research tool for quantitative and qualitative measurements of molecules and bioconjugates at molecular level, because FP is easy to operate for homogenous analysis without the separation of bound and free species from the analytical sample [3–5]. FP detection method, on the other hand, is a relatively inexpensive technique that can be integrated into analysis with a hand-held device [3].

Contamination of the environment with heavy metal ions has been an important worldwide concern for decades [6–8]. Mercury (Hg) is a globally distributed toxic element and can have lethal effects on living systems [9,10]. Because mercury can accumulate in vital organs and tissues, such as the liver, brain, and heart muscle [11,12] and the biomagnification factor could be as much as 10^7 in predatory fish, causing adverse effects in humans and other wildlife that consume fish [13]. It becomes more detrimental after converted to the bioaccumulative form, methylmercury (MeHg) [14]. It has been reported that the upper limits of estimated average dietary exposure to total mercury from foods (e.g. shellfish) is about 0.50 mg kg^{-1} [15]. The U.S. Environmental Protection Agency has set the maximum allowable level of Hg^{2+} in drinking water at 2 ppb [16], and a maximum level of 0.3 μg g^{-1} for fish tissue (wet weight) [17]. Therefore, measurement of accurate level of mercury in food is important in the assessment of mercury exposure risks from food consumption.

For the determination of trace amounts of mercury, various spectroscopic, electrochemical and radiochemical methods were used. The usual methods for the determination of total mercury are atomic spectrometry and molecular mass spectrometry, including atomic absorption spectrometry using the cold vapor method (CVAAS) [18], cold vapor atomic fluorescence spectrometry (CVAFS) [19,20] and inductively coupled plasma mass spectrometry (ICPMS) [21] or liquid chromatography mass spectrometry (LCMS) [22]. Coupling of LC or ICP to MS gained much attention and have been employed to estimate mercury including inorganic mercury and MeHg in fish tissues including muscle, blood and scales [23,24]. It has been reported that the detection limit for MeHg and Hg^{2+} in dogfish tissues was about 9.0 ng g^{-1}

* Corresponding authors. Tel./fax: +86 635 8239 001.
E-mail addresses: yueqiaoli@gmail.com (Q. Yue), liujifeng111@gmail.com (J. Liu).

0039-9140/$ - see front matter © 2013 Elsevier B.V. All rights reserved.
http://dx.doi.org/10.1016/j.talanta.2013.08.017

[25]. However, these methods need expensive and complicate instruments.

FP methods used for the determination of metal ions in food, drinking water and environmental samples are limited. Indeed, there are only a few FP assays which have been used for monitoring Cd^{2+} [26], Pb^{2+} [27], and Hg^{2+} [10]. Herein, a novel biosensor using FP method was constructed for the detection of Hg^{2+} based on the specific interaction between nucleic acid base, thymine (T) and Hg^{2+} to form T–Hg^{2+}–T complex. The formation of T–Hg^{2+}–T complex leads to the increase of molar mass for fluorescence probe due to the binding of fluorophore-labeled T-containing ssDNA to superparamagnetism iron oxide magnetic nanoparticles (MNPs) *via* T–Hg^{2+}–T linkage, thus causing enhancement in FP signals. The FP method developed in this work can be applied into the measurement of total inorganic mercury in canned fish samples.

2. Materials and methods

2.1. Reagents and materials

MNPs of iron oxide which were coated with streptavidin with diameter of 50 nm were purchased from Micromod (GmbH, Germany). Oligonucleotides used in this work were obtained from Sangon (Shanghai Sangon Biotechnology Co., Ltd.). The sequences of ssDNA (Table 1) were 5'–TATTTTATTTTATA-3' and 5'–TATATTT-TATTTTA-3' with biotin and carboxyfluorescein (FAM) labeled on 5'-end, named biotin-linker 1 and FAM-linker 2, respectively, which were put into 95 °C water bath for 10 min and then cooled to room temperature before using for the preparation of stock solutions. Tris(hydroxymethyl)-aminomethane (Tris) and 3-(N-morpholino) propanesulfonic acid (MOPs) were purchased from Fluka (BuchsSwitzerland). $NaNO_3$, NaH_2PO_4, Na_2HPO_4, NaOAc, HOAc and other common metal salts were obtained from Beijing Chemical Works (Beijing, China). The deionized water ($\geq$ 18.2 MΩ) was prepared using a Millipore water system and all chemicals were at least analytical reagent grade.

2.2. Apparatus

All FP data was obtained from a LS 55 spectrofluorometer (Perkin Elmer, USA). The spectrofluorometer is equipped with dichroic mirrors and polarizing filters for fluorescence polarization. Fluorophore labeled ssDNA was employed as the fluorescent probe with the excitation and emission wavelengths at 495 and 515 nm, respectively. The circular dichroism (CD) measurements were obtained on a J-810 CD spectrometer (Jasco, Japan). AFS measurements were obtained on a PF6 atomic fluorescence spectrophotometer (Persee, China). Digestion of the samples was operated in a MDS – 2002AT microwave digester (Sineo Microware Chemical Technology Co. Ltd.). Transmission electron microscope (TEM) images were obtained on a JEM-2100 electron microscope operating at 200 kV (JEOL Ltd., Japan).

Table 1
DNA sequences used in the present work.

Name	Sequences
Biotin-linker 1	5'-Biotin-TATTTTATTTTATA -3'
FAM-linker 2	5'-FAM-TATATTTTATTTTA -3'
Biotin-linker 3	5'-Biotin-TTCGTCTCTGGTGC -3'
FAM-linker 4	5'–FAM-GCTCCTGTGTCGTT -3'
Free labeled-linker 1	5'–TATTTTATTTTATA -3'
Free labeled-linker 2	5'–TATATTTTATTTTA -3'

2.3. Fluorescence polarization

FP is based on the observation of the excitation of fluorescent molecules in solution with plane-polarized light, and the emission comes back into a fixed plane (i.e. the light remains polarized) if the molecules remain stationary during excitation [28]. FP of a molecule is proportional to the molecule's rotational relaxation time. If vertically polarized light excite the fluorophore, the intensity of the emission can be monitored in vertical and horizontal planes. The movement degree of emission from vertical to horizontal plane is related to the mobility of the fluorophore. Based on this detection principle, small molecules rotate quickly during excitation and the emission is depolarized relative to the excitation plane, obtaining lower polarization signals. Large molecules rotate slowly at excited states, resulting in highly polarized emission and high polarization values. The degree of polarization is determined experimentally from measurements of fluorescence intensities parallel and perpendicular with respect to the plane of linearly polarized excitation light, and is expressed in terms of P (measured in millipolarization units, mP). mP value can be calculated by equation Eq. (1),

$$mP = 1000\frac{I_V - GI_H}{I_V + GI_H} \quad (1)$$

where I_V and I_H are the intensity of the emission signal parallel and orthogonal respective to the direction of the electric field of illumination light (determined by the polarizer in the excitation light path), and G is a correction factor of the optical components of the instrument that affects the light beam depending on its polarization plane.

2.4. Titration procedure

0.1 mg ml^{-1} MNPs was prepared directly in 10 mM MOPs solution by dilution of stock solution to 2.0 ml. 0.02 μM biotin-linker 1 was added to MNPs dispersion. They were incubated for about 20 min at room temperature to form MNPs-linker 1. 0.02 μM FAM-linker 2 was then added to MNPs-linker 1 dispersion. Hg^{2+} standard solutions with concentrations ranging from 2.0 nM to 1.0 mM were added to this mixture forming a magnetic system (denoted as MNPs-linker 1 – Hg^{2+} – linker 2). Blank solution of FAM-linker 2 in the presence of MNPs was prepared under the same conditions without Hg^{2+}. The FP increase upon the formation of MNPs-linker 1 – Hg^{2+} – linker 2 complexes was recorded and the enhancement in FP signals (ΔFP) was used to quantify Hg^{2+}.

2.5. Preparation of canned fish samples

Usually, alkaline [29] or acid leaching [30] is used to extract Hg species from biological tissues. To improve the extraction yield, even enzymatic digestion procedures have been used [31]. By comparison, microwave-assisted [32], and ultrasound-assisted extractions [33] provide better extraction efficiency and reduce extraction time and solvent consumption. In this work, microwave-assisted method was used for the digestion of samples, which was operated in a MDS – 2002AT microwave digester equipped with temperature and pressure sensors. Briefly, two canned fish (Tuna and Sadine) with five brands samples were purchased from local market. 1.0 g (wet weight) of five samples were weighted and added to digestion tank containing the mixture of 10 ml concentrated HNO_3 and 2 ml 30% H_2O_2, respectively. And then the digestion tank was introduced in the microwave digester. The whole procedure was finished by five steps with the maximum pressure of 2.5 MPa. After digestion all of the samples were transparent solutions and pH was adjusted to 7.4,

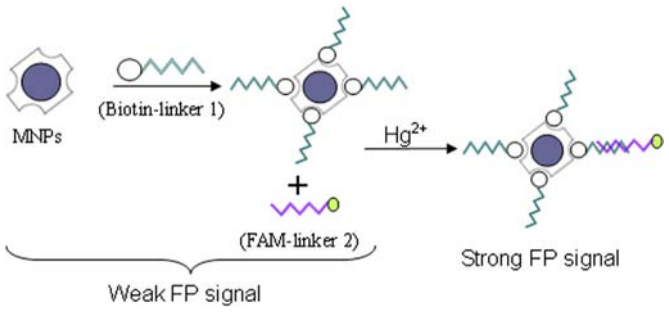

Scheme 1. Schematic construction of a biosensor for Hg^{2+} detection using T–Hg^{2+}–T complexes by FP method.

respectively. In this case, the total inorganic mercury in canned fish samples was transferred to Hg^{2+}. And then the above sample solutions containing Hg^{2+} were used for FP measurements. To confirm the accuracy of the present biosensor for Hg^{2+} detection in canned fish samples, AFS method was employed.

3. Results and discussion

3.1. Working principle

The working principle of the present biosensor is based on the T–Hg^{2+}–T coordination chemistry and upon addition of Hg^{2+} into the T-containing ssDNA, the free ssDNA strands fold from a flexible, disordered state to a structured conformation (Scheme 1) [34]. The T-containing ssDNA which is labeled with biotin can be immobilized on the streptavidin functionalized MNPs and the particles of MNPs-linker 1 are dispersed in the aqueous medium. In the presence of Hg^{2+}, a large molecule as MNPs-linker 1 – Hg^{2+} – linker 2 can be obtained, which increases the molecular weight of FAM-linker 2 and results in the enhanced FP signal [3].

(1) T–Hg^{2+}–T coordination. Due to the high electron density (e.g., σ electron pairs) [35], Hg^{2+} interacts strongly and reversibly with DNA *via* the nitrogen binding sites of purines and pyrimidines [36]. It was noted that a value of binding constant (K_b) of $4.2 \times 10^5\ M^{-1}$ has been reported for Hg^{2+} interacting with two oligonucleotides having two binding sites for Hg^{2+} (i.e., each has two T units) [37]. The formation of folded DNA molecules having T residues in the presence of Hg^{2+} has been confirmed using CD and nuclear magnetic resonance spectroscopy [37]. Moreover, Hg^{2+}-mediated base pair in DNA structure occurs specifically in pyrimidine bases. Namely, T–T mispairs in DNA duplexes selectively capture Hg^{2+} ions, and the metal-mediated T–Hg^{2+}-T base pairs form in DNA duplexes [34].

(2) Magnetic nanoparticles used for FP enhancement. In recent years, because the nanocomposite materials often encompass the desirable features of both organic and inorganic compounds, nanoparticles have gained a great deal of attention due to their unique electronic properties and potential optical-sensing applications [38,39]. Magnetic materials which consist of magnetic nano- or microparticles of iron oxide have wide application in diagnostic and biomedical fields [40], including gene manipulation and immunoassay [16], magnetic resonance imaging (MRI) contrast agents [17], enzyme immobilization [41], and magnetically guided site specific drug delivery agents [42]. It was reported that the detection sensitivity for FP measurement can be significantly improved by the introduction of nanoparticles, e.g. the "gold nanoparticle enhancement" approach had a limit of detection (LOD) of 1.0 nM (0.2 ppb) for Hg^{2+} [10]. Herein, considering the reusability of the present biosensor, MNPs were employed as the FP enhancement probe.

3.2. Optimization of conditions

3.2.1. Effect of MNPs concentration

To optimize the conditions, the influence of the MNPs size and concentration were tested. The linear relationship of the FP vs Hg^{2+} concentration [Hg^{2+}] using 20 nm and 50 nm sized MNPs was carried out and the TEM images for MNPs were illustrated in Fig. S1 (in supporting information), respectively. It was found that the sensitivity with 50 nm sized MNPs was higher than that of 20 nm (data not shown). Therefore, 50 nm MNPs were employed to use in this experiment.

The effect of MNPs concentration was also tested. Firstly, a controlling experiment was carried out using ssDNA aptamers without MNPs. As shown in Fig. 1A, for the tested concentration range of Hg^{2+} (0.2–70 μM) the linearity was not good. Furthermore, MNPs with different concentrations were investigated by comparison of ΔFP value in the presence and absence of 0.5 mM Hg^{2+}. As illustrated in Fig. 1B, MNPs with the concentration of 12.5, 25, 50, 100, and 200 μg ml^{-1} were tested. It can be observed that the value of ΔFP increased with MNPs concentration. And there was no obvious difference in ΔFP value for MNPs with the concentrations of 100 and 200 μg ml^{-1}. So 100 μg ml^{-1} MNPs was used in this work.

3.2.2. Effect of buffer composition and pH

ΔFP at [Hg^{2+}] of 1.0 μM was studied in four buffer systems (10 mM, pH 7.4) including NaH_2PO_4–Na_2HPO_4, Tris–HCl, MOPs and NaOAc-HOAc. The values of ΔFP (mP) for the present four media were 32, 45, 96 and 21, respectively, which showed that the sensitivity for Hg^{2+} detection in the MOPs solution compared with other buffer systems.

To study the effect of pH on Hg^{2+} detection NaOH or HNO_3 solutions were added to the MOPs buffer solution to adjust pH at

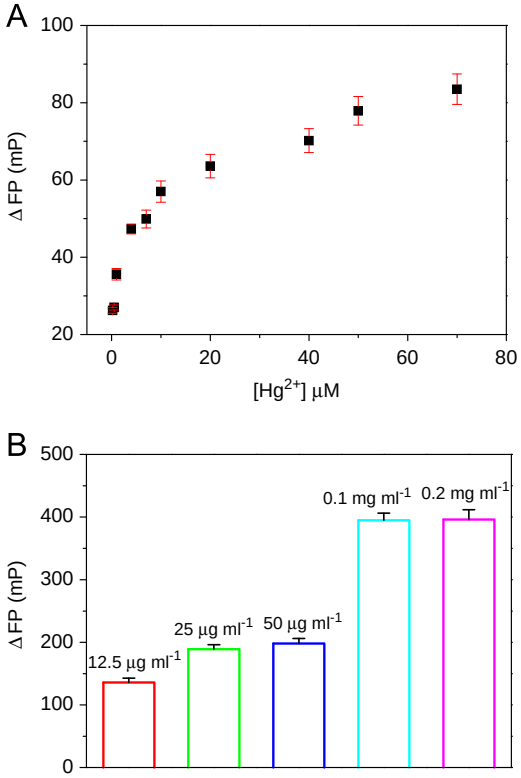

Fig. 1. ΔFP vs [Hg^{2+}] linear relationship using biotin-linker 1 and FAM-linker 2 aptamers in the presence of varying concentration of Hg^{2+} (0.2–70 mM) (A) and the effect of MNPs concentration on ΔFP with [Hg^{2+}] at 0.5 mM (B). The error bars were obtained by three separated measurements.

6.0, 6.5, 7.4, 8.0 and 9.0, respectively. It can be obviously observed that the linear responses of the relative FP value to [Hg^{2+}] were in a good linearity for all of the pH studied (Fig. S2A in supporting information) but the linear slope of the plot at pH 7.4 was the highest, which means that sensitivity for Hg^{2+} detection was highest at pH 7.4. At a pH below 7.4, the protonation of the nitrogen atoms on the thymine base reduces its affinity with Hg^{2+}, while at a higher pH, Hg^{2+} may be associated with OH^-, reducing its complex with DNA. Thus, we chose MOPs with pH 7.4 as the buffer system.

3.2.3. *Effect of $NaNO_3$ concentration*

$NaNO_3$ was employed to adjust the ionic strength of the system. Fig. S2B (in supporting information) illustrated the dependence of the relative FP value vs [Hg^{2+}] in the range of 10.0 – 1.0 mM in the presence of different $NaNO_3$ concentrations (10, 20, 40 and 60 mM) and 20 mM $NaNO_3$ was selected.

3.2.4. *Effect of FAM-linker 2 concentration*

FAM-linker 2 is the FP probe in the constructed sensor system and its concentration (10, 20, 40, 50 and 60 nM) was tested by drawing a linear relationship between relative FP and [Hg^{2+}] (Fig. S3 in supporting information). It can be found that the plot slope obtained from 20 nM FAM-linker 2 was the highest, so the concentration of FAM-linker 2 was set as 20 nM.

3.2.5. *Effect of DNA strands*

In this work, four different strands of T-containing ssDNA were tested (Table 1). Biotin-linker 1 and FAM-linker 2 (L1), biotin-linker 3 and FAM-linker 4 (L2) can hybridize to form dsDNA strands when Hg^{2+} was added to the systems. The formation of the dsDNA strands containing T-Hg^{2+}-T complexes was confirmed by circular dichroism (CD) (Fig. 2A) and UV spectra (Fig. 2B) using free labeled-linker 1 and linker 2 (Table 1). It can be observed that both of the CD and UV spectra of ssDNA red-shifted with the addition of Hg^{2+}, indicating the formation of double helical structure [43]. The linear responses for FP value vs [Hg^{2+}] were obtained using L1 (Fig. 3A) and L2 (Fig. 3B) sensor systems. The former has wider linear range and lower LOD.

3.3. *Selectivity*

The possible interference of other metal ions were studied using Mg^{2+}, Pb^{2+}, Ni^{2+}, Mn^{2+}, Co^{2+}, Ba^{2+}, Cd^{2+}, Al^{3+}, Fe^{3+}, Cd^{3+}, Mg^{2+}, Ca^{2+}, K^+, Na^+ and Zn^{2+} at the concentrations from 1.0 mM to 100 times of the Hg^{2+} (10.0 μM) (Fig. S4 in supporting information). There was a little increase of the FP (mP) value in the presence of other metal ions and this sensor technique has excellent selectivity toward Hg^{2+} over alkali, alkaline earth and other heavy metal ions. It was also demonstrated that different anions had no obvious interferences with the mercury detection (data not shown).

3.4. *Sensitivity and stability of the Hg^{2+} sensor*

Under optimum conditions, different concentrations of Hg^{2+} was titrated according to the general procedure in experimental section, obtaining a linear relationship between ΔFP (mP) and [Hg^{2+}] (Fig. 3A) with a correlation coefficient of 0.9963, and a dynamic range of 2.0 nM–1.0 mM. The LOD was obtained as 0.49 nM according to the recent recommendation of IUPAC as 3.29 S_B/m which derived from the Orange Book in The Analytical Division, where S_B and m were the standard deviation of the blank and slope of the calibration graph, respectively. By comparison with recent publications of Li's [44] and our group [45], the widest

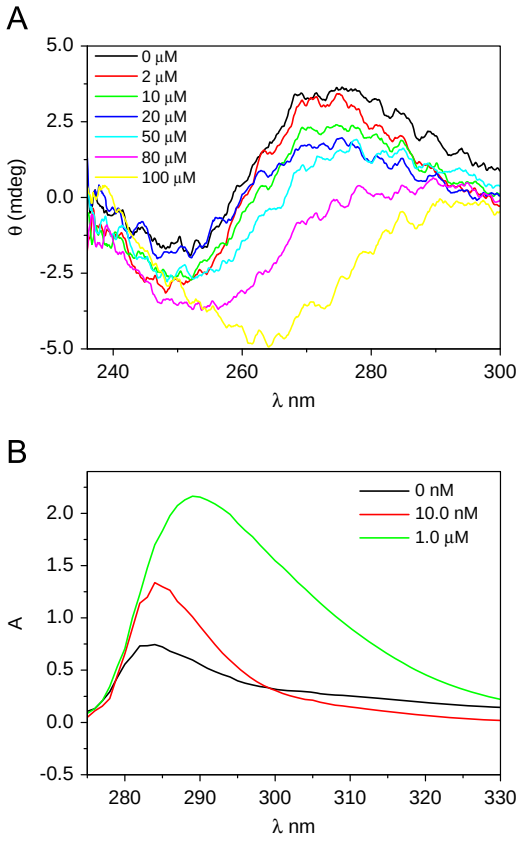

Fig. 2. CD spectra (A) and UV absorption spectra (B) of free labeled-linker 1 and free labeled-linker 2 in the presence of Hg^{2+} with different concentrations (0.0 – 100.0 μM) and (0.0, 10.0 nM, and 1.0 μM), respectively.

linear response range was achieved for the present method. The detection limit of this sensor for Hg^{2+} was as same as that of Li's work although the lower limit of the concentration range was 2.0 nM and 10.0 nM, respectively. In addition, the prior work of our group showed the lowest detection limit.

The stability and reusability of the sensor for Hg^{2+} detection was also tested. The procedure was similar with our previous work [45]. Briefly, appropriate amount of L-cystine was added into the MNPs-linker 1 – Hg^{2+} – linker 2 sensor system to release Hg^{2+} and destroy the T–Hg^{2+}–T structures. MNPs can be collected applying an external magnetic field and reused for Hg^{2+} detection. Usually, the MNPs can be recycled for 6 cycling times without obvious deterioration in Hg^{2+} detection (Fig. S5 in supporting information).

3.5. *Hg^{2+} detection in canned fish Samples*

To investigate the feasibility of the present sensor for Hg^{2+} detection in real samples, Hg^{2+} level in canned fish samples was also measured with AFS method. Preparation of samples was carried out according to the general experimental procedures, and a simple and rapid microwave-assisted extraction procedure was used. Five samples of different brands were tested including 2 tuna and 3 sadine canned fish samples, which were digested in the mixture of concentrated HNO_3 and H_2O_2 to release inorganic mercury (Hg^{2+}) in samples [24]. Hg^{2+} in the samples was then detected using the sensor technique developed in this work. As shown in Table 2, the Hg^{2+} level obtained from the FP sensor technique agrees well with that of AFS method, demonstrating the potential of this FP sensor technique of real samples' analysis.

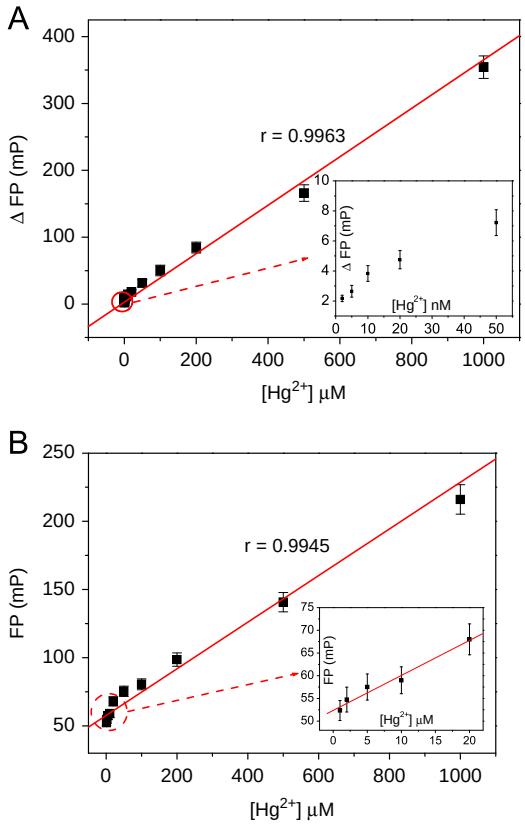

Fig. 3. Linear responses of the magnetic system using biotin-linker 1 and FAM-linker 2 (A) and biotin-linker 3 and FAM-linker 4 aptamers (B) in the presence of varying concentration of Hg^{2+} (2.0 nM – 1.0 mM and 1.0 μM – 1.0 mM), respectively. The inset displays Hg^{2+} concentration in the range of 2.0 – 50.0 nM and 1.0 μM – 20.0 μM, respectively. The error bars were obtained by three separated measurements.

Table 2
Determination of Hg^{2+} in canned fish samples using the proposed method and AFS[a].

Sample	Added	Mean[b] + RSD[c]	AFS + RSD
Tuna sample 1#	0	8.8 ± 0.3	8.7 ± 0.5
	50	59.2 ± 0.9	59.0 ± 1.2
Tuna sample 2#	0	240.1 ± 2.4	234.2 ± 2.6
Sadine sample 1#	0	30.1 ± 0.6	29.7 ± 0.7
	50	80.5 ± 1.5	78.9 ± 1.3
Sadine sample 2#	0	7.3 ± 0.3	7.2 ± 0.3
	50	57.0 ± 0.8	58.0 ± 1.0
Sadine sample 3#	0	–	–
	50	50.1 ± 0.7	50.2 ± 0.6

"–" represented the sample was not detectable. Concentration: MNPs, 100 μg ml^{-1}; MOPs, 10 mM; $NaNO_3$, 0.02 M; pH 7.4.

[a] The concentration of Hg^{2+} at nM level;
[b] Mean of three separated measurements;
[c] RSD, relative standard deviation;

4. Conclusions

In summary, a fast, simple and accurate FP method for mercury sensing has been developed, which can be applicable for total mercury detection in real samples. The approach was realized by combining T–Hg^{2+}–T coordination chemistry and FP method using MNPs as enhancement probe. Due to the high specific interaction between T and Hg^{2+}, a good selectivity and accuracy for Hg^{2+} detection was achieved. This method has been successfully applied to determine total inorganic mercury in the canned fish samples after microwave-assisted digestion.

Acknowledgment

This work was supported by Natural Science Foundation of China for Funding (21005036, 20875042, 21075058, 21127006), Natural Science Foundation (ZR2010BZ004, JQ201307, JQ201106) of Shandong Province and Research Fund of Shandong Academy of Agricultural Sciences.

Appendix A. Supplementary materials

Supplementary data associated with this article can be found in the online version at http://dx.doi.org/10.1016/j.talanta.2013.08.017.

References

[1] F. Perrin, J. Phys. Radium 7 (1926) 390–401.
[2] G. Weber, in: Elli Kohen (Ed.), From Solution Spectroscopy to Image Spectroscopy. In Cell Structure and Function by Microspectrofluorometry, Academic Press, Inc., New York, 1989, pp. 71–85.
[3] J.A. Cruz-Aguado, G. Penner, Anal. Chem 80 (2008) 8853–8855.
[4] H. Härmä, G. Sarrail, J. Kirjavainen, E. Martikkala, I. Hemmila, P. Hänninen, Anal. Chem. 82 (2010) 892–897.
[5] P. Otero, A. Alfonso, C. Alfonso, R. Aráoz, J. Molgó, M.R. Vieytes, L.M. Botana, Anal. Chim. Acta 701 (2011) 200–208.
[6] G.K. Darbha, A. Ray, P.C. Ray, ACS Nano 1 (2007) 208–214.
[7] M. Pal, S. Ghosh, M. Mukhopadhyay, M. Ghosh, Environ. Monit. Assess. 184 (2012) 3407–3414.
[8] D.X. Soto, R. Roig, E. Gacia, J. Catalan, Environ. Pollut 159 (2011) 1481–1489.
[9] M.J. Yuan, Y.L. Li, J.B. Li, C.H. Li, X.F. Liu, J. Lv, J.L. Xu, H.B. Liu, S. Wang, D.B. Zhu, Org. Lett. 9 (2007) 2313–2316.
[10] B.-C. Ye, B.C. Yin, Angew. Chem. Int. Ed. 47 (2008) 8386–8389.
[11] G.K. Darbha, A.K. Singh, U.S. Rai, E. Yu, H.T. Yu, C.P. Ray, J. Am. Chem. Soc. 130 (2008) 8038–8043.
[12] H. Yang, Z.Q. Tian, J.J. Wang, S.Q. Yang, Sens. Actuators B 161 (2012) 429–433.
[13] K. Murata, P. Grandjean, M. Dakeishi, Am. J. Ind. Med. 50 (2007) 765–771.
[14] C.A. Eagles-Smith, J.T. Ackerman, Environ. Sci. Technol 43 (2009) 8658–8664.
[15] S. Clémens, M. Monperrus, O.F.X. Donard, D. Amouroux, T. Guérin, Talanta 89 (2012) 12–20.
[16] H. Nakayama, A. Arakaki, K. Maruyama, H. Takeyama, T. Matsunaga, Biotechnol. Bioeng 84 (2003) 96–102.
[17] O. Osman, L.F. Zanini, M. Frénéa-Robin, F. Dumas-Bouchiat, N.M. Dempsey, G. Reyne, F. Buret, N. Haddour, Biomed. Microdevices 14 (2012) 947–954.
[18] J. Gómez-Ariza, F. Lorenzo, T. García-Barrera, Anal. Bioanal. Chem 382 (2005) 485–492.
[19] W. Geng, T. Nakajima, H. Takanashi, A. Ohki, J. Hazard. Mater 154 (2008) 325–330.
[20] Y.L. Yu, Z. Du, J.H. Wang, J. Anal. At. Spectrom 22 (2007) 650–656.
[21] K. Leopold, M. Foulkes, P. Worsfold, Anal. Chim. Acta 663 (2010) 127–138.
[22] M. Leermakers, W. Baeyens, P. Quevauviller, M. Horvat, Trends Anal. Chem 24 (2005) 383–393.
[23] D. Esteban-Fernández, M. Mirat, M.I.M. de la Hinojosa, J.I.G. Alonso, J. Agric. Food Chem 60 (2012) 8333–8339.
[24] L.-Y. Lin, L.-F. Chang, S.-J. Jiang, J. Agric. Food Chem 56 (2008) 6868–6872.
[25] Á. Castillo, P. RodrÍguez-González, G. Centineo, A.F. Roig-Navarro, J.I.G. Alonso, Anal. Chem 82 (2010) 2773–2783.
[26] D.K. Johnson, Anal. Chim. Acta 399 (1999) 161–172.
[27] D.K. Johnson, Comb. Chem. High Throughput Screen 6 (2003) 245–255.
[28] J.R. Lakowicz, Principles of Fluorescence Spectroscopy, Third Edition, Springer, New York, USA, 2006.
[29] J.J.B. Nevado, R.C.R. Martín-Doimeadios, F.J.G. Bernardo, M.J. Moreno, J. Chromatogr. A 1093 (2005) 21–28.
[30] H. Hintelmann, H.T. Nguyen, Anal. Bioanal. Chem 381 (2005) 360–365.
[31] L. Ebdon, M.E. Foulkes, S. Le Roux, R. Muñoz-Olivas, Analyst 127 (2002) 1108–1114.
[32] W.C. Davis, S.S.V. Pol, M.M. Schantz, S.E. Long, R.D. Day, S.J. Christopher, J. Anal. At. Spectrom. 19 (2004) 1546–1551.
[33] B.L. Batista, J.L. Rodrigues, S.S. de Souza, V.C.O. Souza, F.B. Jr., Food Chem 126 (2011) 2000–2004.
[34] A.A. Voityuk, Electronic Coupling Mediated by Stacked [Thymine-Hg-Thymine] Base Pairs, J. Phys. Chem. B 110 (2006) 21010–21013.
[35] T.T. Baby, S. Ramaprabhu, Talanta 80 (2010) 2016–2022.
[36] D.W. Gruenwedel, M.K. Cruikshank, DNA Mercury-induced, Biochemistry 29 (1990) 2110–2116.
[37] C.-K. Chiang, C.-C. Huang, C.-W. Liu, H.-T. Chang, Anal. Chem. 80 (2008) 3716–3721.
[38] C.C. Huang, Z.S. Yang, K.H. Lee, H.T. Chang, Angew. Chem. Int. Ed. 46 (2007) 6824–6828.
[39] U. Drechsler, B. Erdogan, V.M. Rotello, Chem. Eur. J 10 (2004) 5570–5579.
[40] B.M. Novak, Adv. Mater 5 (1993) 422–433.
[41] L.Y. Xue, X.M. Zhou, D. Xing, Chem. Commun 46 (2010) 7373–7375.

[42] A.P. Fan, C.W. Lau, J.Z. Lu, Anal. Chem. 77 (2005) 3238–3242.
[43] Y. Miyake, H. Togashi, M. Tashiro, H. Yamaguchi, S. Oda, M. Kudo, Y. Tanaka, Y. Kondo, R. Sawa, T. Fujimoto, T. Machinami, A. Ono, J. Am. Chem. Soc. 128 (2006) 2172–2173.
[44] J.R. Zhang, W.T. Huang, W.Y. Xie, T. Wen, H.Q. Luo, N.B. Li, Analyst 37 (2012) 3300–3305.
[45] Q.L. Yue, T.F. Shen, J.T. Wang, L. Wang, S.L. Xu, H.B. Li, J.F. Liu, Chem. Commun. 49 (2013) 1750–1752.